Supporting Information S1 Appendix

1 Fluid dynamics simulation

1.1 Model and discretization

As discussed in Methods, the Stochastic Immersed Boundary method formulates the fluid in Eulerian coordinates, which we discretize in a regular Cartesian grid, and the membranes in Eulerian coordinates, which we discretize into a triangular mesh. We describe the membranes using the Helfrich energy functional (1),

$$\Phi_{bend}(\mathbf{X}) = \frac{\kappa_B}{2}\int_{\mathcal{S}} H^2 dA, \tag{1}$$

where κ_B is bending rigidity, H is mean curvature of the membrane surface, and $\mathcal{S}$ is the membrane domain, parameterized by s. In the discrete scheme, the curvature reads as

$$\mathbf{H}^{(k)} = -\sum_{l\in\tau(k)} \frac{1}{2}(\mathbf{n}_l \times \mathbf{E}_l^k) \tag{2}$$

Here k parameterizes the vertex of the triangular mesh, $\tau(k)$ is the set of indices of triangles that touch vertex $\mathbf{X}_k$. The area associated with vertex k is then

$$A^{(k)} = \frac{1}{3}\sum_{l\in\tau(k)} \text{Area}(T_l) \tag{3}$$

The total discrete bending energy is given by

$$\Phi_{bend} = \frac{\kappa_b}{2}\sum_{k=1}^{N_v} \frac{\left\|\mathbf{H}^{(k)}\right\|^2}{A^{(k)}}, \tag{4}$$

where N_v is the total number of vertex on the mesh. The force on each node arising from bending resistance is then

$$\mathbf{F}(\mathbf{X}_k) = -\frac{\partial \Phi_{bend}}{\partial \mathbf{X}_k} \tag{5}$$

$$= \frac{\kappa_b}{2}\sum_{l\in\tau(k)} \left(\left(\bar{H}_l - \mathbf{n}_l\cdot\mathbf{C}_l\right)\left(\frac{1}{2}\mathbf{n}_l\times\mathbf{E}_l^k\right) + \frac{1}{2}\mathbf{C}_l\times\mathbf{E}_l^k + \mathbf{n}_l\times\mathbf{h}_l^k\right), \tag{6}$$

where $\mathbf{E}_l^k$ is the side vector against vertex k in the triangle l that includes vertex k, and

$$\begin{cases} \bar{H}_l = \frac{1}{3}\sum_{p\in V(l)} \frac{\left\|\mathbf{H}^{(p)}\right\|^2}{\left(A^{(p)}\right)^2}; \\ \mathbf{C}_l = \frac{1}{A_l}\sum_{p\in V(l)} \mathbf{E}_p \times \frac{\mathbf{H}^{(p)}}{A^{(p)}}; \\ \mathbf{h}_l^k = \frac{\mathbf{H}_k^{(l,3)}}{A_k^{(l,3)}} - \frac{\mathbf{H}_k^{(l,2)}}{A_k^{(l,2)}}; \end{cases} \tag{7}$$

where $V(l)$ is the set of triangles include vertex k, and the notations $()_k^{(l,3)}$ and $()_k^{(l,2)}$ denote the two vertexes other than k in triangle l in clockwise order.

In addition to the bending energy, we consider a membrane that resists stretch by a surface tension energy

$$\Phi_{tension}[\mathbf{X}] = \sigma_0\int_{\mathcal{S}} \left(\frac{dA - dA_0}{dA_0}\right)^2 dA_0 \tag{8}$$

where σ_0 is the surface tension constant. In the discrete scheme, the surface tension energy reads as

$$\Phi_{tension} = \sigma_0\sum_l \left(\frac{A_l(t) - A_l(0)}{A_l(0)}\right)^2 A_0(t). \tag{9}$$

The force on each node arising from surface tension is

$$\mathbf{F}_{tension}(\mathbf{X}_k) = -\frac{\partial \Phi_{tension}}{\partial \mathbf{X}_k}, \tag{10}$$

$$= \frac{\sigma_0}{2} \sum_{l \in \tau(k)} \left(\frac{A_l(t) - A_l(0)}{A_l(0)} \right) \mathbf{n}_l \times \mathbf{E}_l^k. \tag{11}$$

Finally, the membrane resists shear by a two-dimensional neo-Hookean energy (2). Let $\mathbf{Z}(\mathbf{q}, t) \in \mathcal{R}^3$ be the reference configuration, and $\mathbf{X}(\mathbf{q}, t)$ the current deformed configuration. the two-dimensional neo-Hookean shear potential is

$$\Phi_{shear}[\mathbf{X}] = \frac{\kappa_s}{2} \int_{\mathcal{S}} \left(\text{trace}(G G_0^{-1}) \left(\frac{\det G}{\det G_0} \right)^{-1/2} - 2 \right) (\det G_0)^{1/2} \, d\mathbf{q}, \tag{12}$$

where κ_s is the shear modulus of the membrane. Here the Cauchy-Green deformation tensors are defined as

$$G = \left(\frac{\partial \mathbf{X}}{\partial \mathbf{q}} \right)^T \left(\frac{\partial \mathbf{X}}{\partial \mathbf{q}} \right), \quad G_0 = \left(\frac{\partial \mathbf{Z}}{\partial \mathbf{q}} \right)^T \left(\frac{\partial \mathbf{Z}}{\partial \mathbf{q}} \right). \tag{13}$$

The discrete shear energy of triangle l reads as

$$\Phi_{shear}(T_l) = \kappa_s \left(\frac{\|\mathbf{X}_{13}\|^2 \|\mathbf{Z}_{23}\|^2 - 2 (\mathbf{X}_{13} \cdot \mathbf{X}_{23}) (\mathbf{Z}_{13} \cdot \mathbf{Z}_{23}) + \|\mathbf{X}_{23}\|^2 \|\mathbf{Z}_{13}\|^2}{8 Area(T_{\mathbf{X},l})} \right) - \kappa_s Area(T_{\mathbf{Z},l}). \tag{14}$$

So the force can be found as

$$\mathbf{F}_1 = -\kappa_s \frac{\|\mathbf{Z}_{23}\|^2 \mathbf{X}_{13} - 2 (\mathbf{Z}_{23} \cdot \mathbf{Z}_{13}) \mathbf{X}_{23}}{4 Area(T_{\mathbf{X},l})} - \kappa_s' \frac{\|\mathbf{X}_{23}\|^2 \mathbf{X}_{13} - 2 (\mathbf{X}_{23} \cdot \mathbf{X}_{13}) \mathbf{X}_{23}}{4 Area(T_{\mathbf{X},l})} \tag{15}$$

$$\mathbf{F}_2 = -\kappa_s \frac{\|\mathbf{Z}_{23}\|^2 \mathbf{X}_{33} - 2 (\mathbf{Z}_{23} \cdot \mathbf{Z}_{13}) \mathbf{X}_{23}}{4 Area(T_{\mathbf{X},l})} - \kappa_s' \frac{\|\mathbf{X}_{23}\|^2 \mathbf{X}_{33} - 2 (\mathbf{X}_{23} \cdot \mathbf{X}_{13}) \mathbf{X}_{23}}{4 Area(T_{\mathbf{X},l})} \tag{16}$$

$$\mathbf{F}_3 = -\kappa_s \frac{\|\mathbf{Z}_{22}\|^2 \mathbf{X}_{31} - 2 (\mathbf{Z}_{21} \cdot \mathbf{Z}_{31}) \mathbf{X}_{21}}{4 Area(T_{\mathbf{X},l})} - \kappa_s' \frac{\|\mathbf{X}_{21}\|^2 \mathbf{X}_{31} - 2 (\mathbf{X}_{21} \cdot \mathbf{X}_{31}) \mathbf{X}_{21}}{4 Area(T_{\mathbf{X},l})} \tag{17}$$

where

$$\kappa_s' = -\frac{\kappa_s}{8} \left(\frac{\|\mathbf{X}_{13}\|^2 \|\mathbf{Z}_{23}\|^2 - 2 (\mathbf{X}_{13} \cdot \mathbf{X}_{23}) (\mathbf{Z}_{13} \cdot \mathbf{Z}_{23}) + \|\mathbf{X}_{23}\|^2 \|\mathbf{Z}_{13}\|^2}{Area(T_{\mathbf{X},l})^2} \right) \tag{18}$$

1.2 Numerical implementation

We use Eulerian and Lagrangian reference frames for the fluid and structure, respectively (2, 3). The Eulerian fluid domain $\{\mathbf{x} | \mathbf{x} \in \Omega\}$ is resolved by a finite difference discretization. The fluid variables (velocity field $\mathbf{u}$ and pressure field p) are represented on a periodic grid with length L along each direction, N grid points along each direction, and grid spacing $\Delta x = L/N$. The discrete Fourier transform of the fluid variables are

$$\hat{\mathbf{u}}_{\mathbf{k}} = \frac{1}{N^3} \sum_{\mathbf{m}} \mathbf{u}_{\mathbf{m}} e^{-2\pi i \mathbf{k} \cdot \mathbf{m}/N}. \tag{19}$$

$$\mathbf{u}_{\mathbf{m}} = \sum_{\mathbf{k}} \hat{\mathbf{u}}_{\mathbf{k}} e^{2\pi i \mathbf{k} \cdot \mathbf{m}/N}. \tag{20}$$

Here each sum runs over the N^3 lattice points defined by $\mathbf{m} = \{m_1, m_2, m_3\}$ and $\mathbf{k} = \{k_1, k_2, k_3\}$, where $0 \le m_i \le N-1$ and $0 \le k_i \le N-1$ for $i = 1, 2, 3$. The membranes in the Lagrangian domain $\{\mathbf{X} | \mathbf{X} \in \mathcal{S}\}$ are also resolved by a evenly spaced finite difference discretization.

Solving unsteady Stokes equations in the Fourier space, the velocity is (2, 4)

$$\hat{\mathbf{u}}_{\mathbf{k}}(t^{n+1}) = \hat{\mathbf{u}}_{\mathbf{k}}(t^n) e^{-\alpha_{\mathbf{k}} \Delta t} + \frac{(1 - e^{-\alpha_{\mathbf{k}} \Delta t})}{\rho \alpha_{\mathbf{k}}} \xi_{\mathbf{k}} \hat{\mathbf{f}}_{\mathbf{k}} + \sqrt{2 D_{\mathbf{k}}} \xi_{\mathbf{k}} \int_{t^n}^{t^{n+1}} e^{-\alpha_{\mathbf{k}} (t^{n+1} - s)} d\tilde{B}_{\mathbf{k}}(s), \tag{21}$$

where

$$\alpha_{\mathbf{k}} = \frac{2\eta}{\rho \Delta x^2} \sum_{l=1}^{3} \left[1 - \cos\left(2\pi \mathbf{k}^{(l)}/N\right)\right], \tag{22}$$

and $\xi_{\mathbf{k}} = I - \hat{\mathbf{g}}_{\mathbf{k}} \cdot \hat{\mathbf{g}}_{\mathbf{k}}^T / |\hat{\mathbf{g}}_{\mathbf{k}}|^2$ is the projection orthogonal to $\hat{\mathbf{g}}_{\mathbf{k}}$, defined by

$$\hat{\mathbf{g}}_{\mathbf{k}} = \sin\left(2\pi \mathbf{k}^{(l)}/N\right)/\Delta x, \tag{23}$$

which is used to enforce the incompressibility constraint. The strength of the thermal fluctuation is described by $D_{\mathbf{k}}$, which is (2, 4)

$$D_{\mathbf{k}} = \begin{cases} \frac{k_B T}{2\rho L^3} \alpha_{\mathbf{k}}, & \text{for } \mathbf{k} \in \mathcal{H}, \\ \frac{k_B T}{\rho L^3} \alpha_{\mathbf{k}}, & \text{for } \mathbf{k} \notin \mathcal{H}. \end{cases} \tag{24}$$

Here $\mathcal{H} = \{\mathbf{k} | k_i = 0, N/2, i = 1, 2, 3\}$. The average velocity $\mathbf{u}_1$ is obtained by a discrete inverse fast Fourier transform (IFFT) of appropriately generated random variables $\hat{\mathbf{u}}_{\mathbf{k}}$ in Fourier space, where

$$\hat{\mathbf{u}}_{\mathbf{k}} = -\frac{\sqrt{2D_{\mathbf{k}}}}{\alpha_{\mathbf{k}} \Delta t} \int_{t^n}^{t^{n+1}} e^{-\alpha_{\mathbf{k}}(t^{n+1}-u)} \xi_{\mathbf{k}} d\tilde{B}_{\mathbf{k}}(u) + \frac{\sqrt{2D_{\mathbf{k}}}}{\alpha_{\mathbf{k}} \Delta t} \left(\xi_{\mathbf{k}} \hat{B}_{\mathbf{k}}(t_{n+1}) - \xi_{\mathbf{k}} \hat{B}_{\mathbf{k}}(t_n)\right). \tag{25}$$

With this, the structure is then updated by

$$\mathbf{X}^{n+1,(k)} = \mathbf{X}^{n,(k)} + \sum_{\mathbf{m}} \delta_c(\mathbf{x}_{\mathbf{m}} - \mathbf{X}^{\mathbf{n},k}) h^3 \hat{\mathbf{H}}_{\mathbf{k}}. \tag{26}$$

where $t_n = n\Delta t$, and Δt is the step size.

Finally the displacement of the fluid $\hat{\mathbf{H}}_{\mathbf{k}}$ is

$$\hat{\mathbf{H}}_{\mathbf{k}} = \left(\frac{1 - e^{-\alpha_{\mathbf{k}} \Delta t}}{\alpha_k}\right) \hat{\mathbf{u}}_{\mathbf{k}}^n - \frac{1}{\alpha_k} \left(\sqrt{2D_{\mathbf{k}}} \int_{t^n}^{t^{n+1}} e^{-\alpha_{\mathbf{k}}(t+\Delta t-s)} \xi_{\mathbf{k}} d\mathbf{B}_{\mathbf{k}}(s)\right) + \frac{\sqrt{2D_{\mathbf{k}}}}{\alpha_k} \left(\xi_{\mathbf{k}} \mathbf{B}_{\mathbf{k}}(t^{n+1}) - \xi_{\mathbf{k}} \mathbf{B}_{\mathbf{k}}(t^n)\right). \tag{27}$$

The covariance structure of $\int_{t^n}^{t^{n+1}} e^{-\alpha_{\mathbf{k}}(t-s)} \xi_{\mathbf{k}} d\mathbf{B}_{\mathbf{k}}(s)$ and $\left(\xi_{\mathbf{k}} \mathbf{B}_{\mathbf{k}}(t^{n+1}) - \xi_{\mathbf{k}} \mathbf{B}_{\mathbf{k}}(t^n)\right)$ reads as

$$\mathbb{E}\left[\mathrm{Re}\left(\int_{t^n}^{t^{n+1}} e^{-\alpha_{\mathbf{k}}(t^{n+1}-s)} d\mathbf{B}_{\mathbf{k}}(s)\right) \mathrm{Re}\left(\mathbf{B}_{\mathbf{k}}(t^{n+1}) - \mathbf{B}_{\mathbf{k}}(t^n)\right)\right] = \frac{1}{\alpha_{\mathbf{k}}}(1 - e^{-\alpha_{\mathbf{k}} \Delta t}). \tag{28}$$

We refer to (2) for more details about the discretization of the bending energy, surface energy, and the corresponding elastic force.

The fluid domain is a rectangular box of $512 \times 512 \times 192$, where the spatial size $\Delta x = 5$ nm. The average of the side length of the triangular mesh is $\Delta L = 10$ nm. We set the time step $\Delta t = 0.5$ ns. We used NVIDIA GPU Tesla K40 and Geforce 1080 Ti. The average machine time cost per step is 0.1 s, and the CUDA C/C++ program is 5-10 times faster than the MATLAB version.

2 Rare event simulation

2.1 Overview of rare event simulation method

The Weighted Ensemble (WE) algorithm (5) is a method for efficient simulation of rare events. The method is broadly applicable to stochastic dynamic models and simulation engines (6). Details of the methodology are discussed in a recent review (7) and references therein. Briefly, the algorithm works as follows: state-space is divided up into bins that span rare transitions of interest, along a progress coordinate (λ). Initially, a single simulation trajectory, or "replica", is assigned a weight of 1 and allowed to freely move within and between bins for a user-defined lagtime τ_{WE}. After each iteration of τ_{WE}, a splitting and culling procedure divides and/or combines replicas and their associated weights in such a way as to reach and maintain an approximately equal number of weighted replicas, M, in each bin. Over the course of the simulation, the combined weights of the replicas in a bin (averaged over successive iterations) will evolve toward the steady-state probability of the system to reside in that bin. The mean first passage time from an initial region of interest A to a target region B is obtained as

$$\mathrm{MFPT}_{A \to B} = \frac{1}{\overline{\Phi}_{A \to B}}, \tag{29}$$

where $\overline{\Phi}_{A\to B}$ is the is the steady-state, time-averaged probability flux into region B of trajectories that were previously in A. This flux is estimated from the weights of replicas that successfully reach the target B; upon reaching the target, these weights are then immediately reintroduced into region A for the next simulation iteration.

By maintaining even sampling in each bin, with weights proportional to probability, the algorithm essentially redistributes computational effort from high- to low-probability regions. The method furthermore increases efficiency by capitalizing on incremental progress of replicas toward the target in many, short-time simulations. By contrast, conventional simulation requires long waiting-times for individual trajectories to fully complete a rare transition of interest.

2.2 Simulation of rare events in Ornstein-Uhlenbeck process

Although several variants of the WE method exists (7), we use the original implemenation by Huber and Kim (5), which is often termed the out-of-equilibrium method because replicas which enter B are continuously reintroduced into A.

To model the full fluid dynamics simulations presented in the Main Text, we use a one-component Ornstein-Uhlenbeck (OU) process to describe a single membrane,

$$dZ = \frac{1}{\tau} Z dt + \frac{\sigma}{\sqrt{\tau}} dW, \tag{30}$$

and a two-component OU process to describe the interface,

$$dX = \frac{1}{\tau_{\text{slow}}} X dt + \frac{\sigma}{\sqrt{\tau_{\text{slow}}}} dW_1, \tag{31}$$

$$dY = \frac{1}{\tau_{\text{fast}}} Y dt + \frac{\sigma}{\sqrt{\tau_{\text{fast}}}} dW_2, \tag{32}$$

$$Z = cX + \sqrt{1-c^2} Y. \tag{33}$$

For the one- and two-component OU process, the progress coordinate λ is given by $Z(t)$. The target region B is defined as $Z(t) \geq Z^*$ and A is any $Z(t) < Z^*$. The binning strategy, number of replicas per bin (M) and iteration time (τ_{WE}) were chosen through trial simulations in such a way as to maximize simulation efficiency while minimizing iteration-to-iteration fluctuations of the estimated flux, $\Phi_{A\to B}$. The WE code was implemented in MATLAB. Simulation parameters are given in Table 1.

Table 1: Ornstein-Ulhenbeck approximation parameters and Weighted Ensemble computational parameters used to approximate mean first-passage times

	Model Parameters	Simulation Parameters
One-component OU	$\sigma = 3.1385$ nm,	$dt = 1.0 \times 10^{-9}$
	$\tau_{OU} = 1.05 \times 10^{-6}$	
	$Z^* = \{9, 20, 30, 40, 50\}$	$\tau_{WE} = 1.0 \times 10^{-8}$, $M = 32$, Bins= $[-\infty, 0 : 0.1 : Z^*]$
Two-component OU	$\sigma = 4.27$ nm	$dt = 1.0 \times 10^{-9}$
	$\tau_{\text{slow}} = 8.18 \times 10^{-5}$ nm,	
	$\tau_{\text{fast}} = 5.22 \times 10^{-7}$ nm	
	$Z^* = 9$	$\tau_{WE} = 1.0 \times 10^{-8}$, $M = 200$, Bins=$[-\infty, 0 : 0.1 : 9]$
	$Z^* = 15$	$\tau_{WE} = 1.0 \times 10^{-8}$, $M = 200$, Bins=$[-\infty, 0 : 0.3 : 15]$
	$Z^* = \{20, 25\}$	$\tau_{WE} = 1.0 \times 10^{-8}$, $M = 200$, Bins=$[-\infty, 0 : 0.3 : 15, 15.3 : .1 : Z^*]$

2.3 Weighted Ensemble results

We applied the Weighted Ensemble algorithm to the one-component and two-component OU processes with parameters in Table 1. The one-component calculations show good agreement (Main Text Fig. 4) to an analytical approximation (8) for the MFPT of a simple OU process starting from $Z_0 = 0$ to reach $Z(t) \geq Z^*$, specifically

$$\text{MFPT}(Z^*) = \tau\sqrt{2\pi} \int_0^{Z^*/\sigma} \mathrm{e}^{u^2/2} du. \tag{34}$$

As a validation, we simulate the two-component process at various values of c. The fraction of the process driven

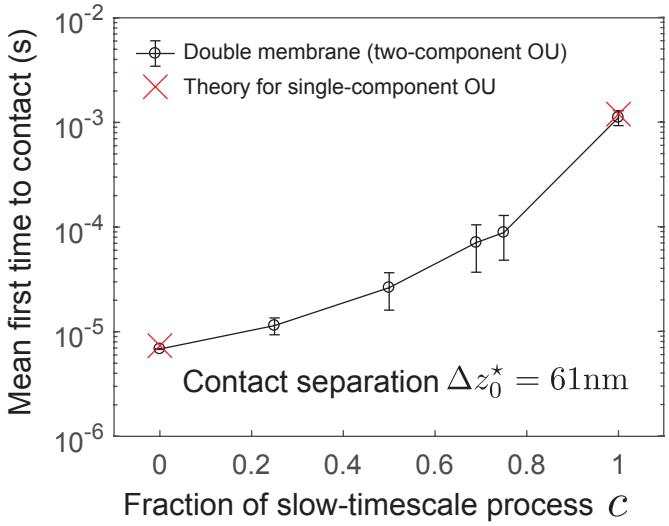

Figure 1: Validation of MFPTs for two-component OU at $Z^\star = 9\text{nm}$ (corresponding to $\Delta z_0^\star = 61\text{nm}$. Red crosses indicate analytical results from (8).

by the slow process, c (defined in Eq. 33), dictates the MFPT. In addition, since $c = 0$ and $c = 1$ are effectively single-component OU processes, we can validate our computation with the theoretical MFPTs from (8).

References

[1] Helfrich W. Elastic properties of lipid bilayers: theory and possible experiments. Z Naturf C. 1973;28:693–703.

[2] Wu CH, Fai TG, Atzberger PJ, Peskin CS. Simulation of osmotic swelling by the stochastic immersed boundary method. SIAM J Sci Comp. 2015;37(4):B660–B688.

[3] Atzberger P. Stochastic Eulerian Lagrangian Methods for Fluid Structure Interactions with Thermal Fluctuations. J Comp Phys. 2011;230:2821–2837.

[4] Atzberger PJ. A note on the correspondence of an immersed boundary method incorporating thermal fluctuations with Stokesian-Brownian dynamics. Physica D. 2007;226:144–150.

[5] Huber GA, Kim S. Weighted-ensemble Brownian dynamics simulations for protein association reactions. Biophys J. 1996;70(1):97–110.

[6] Zhang BW, Jasnow D, Zuckerman DM. The weighted ensemble path sampling method is statistically exact for a broad class of stochastic processes and binning procedures. J Chem Phys. 2010;132(5):054107.

[7] Zuckerman DM, Chong LT. Weighted Ensemble Simulation: Review of Methodology, Applications, and Software. Annu Rev Biophysics. 2017;46(1):43–57.

[8] Thomas MU. Some mean first-passage time approximations for the Ornstein-Uhlenbeck process. J Applied Probability. 1975;12(3):600–604.